Preparing to Measure Vacuum Magnetic Birefringence: Measuring Cavity Birefringence

Mary Ann Cahoon

University of Florida- Department of Physics

July 31, 2019

Abstract

Vacuum magnetic birefringence (VMB) is predicted by quantum electrodynamics (QED), but, because of the exceedingly small scale of the predicted effect, has yet to be experimentally confirmed. The anisotropy of the QED vacuum structure causes a change in the polarization of light propagating in a high magnetic field. The proposed experiment to find axion like particles in the Any Light Particle Search (ALPS) can be used to measure VMB. This paper describes a sensing method to measure the birefringence of an optical cavity, and a table-top experimental test-bed to study systematic, non-VMB signals that might limit the detection sensitivity . A Fabry-Perot cavity was built and aligned. Light from two 1064 nm lasers was coupled into a single mode fiber and mode matched with lenses to the cavity. Time dependent birefringence was injected in the cavity using an auxillary short Fabry-Perot cavity with a piezo actuated end mirror. One laser was locked to the cavity using Poind-Drever-Hall (PDH) locking, while the second laser was locked to a 25MHz frequency offset using a heterodyne phase lock loop (PLL). Preliminary testing showed that the time dependent birefringence was generated at the expected frequency . Future testing will find the relationship between the modulated birefringence in the cavity and the measured signal.

Introduction

Vacuum magnetic birefringence (VMB) is one of the oldest unconfirmed predictions of quantum electrodynamics (QED) [1]. QED predicts that, in the presence of a high magnetic field, the vacuum exhibits birefringent properties [2]. Birefringence is a property typically found in anisotropic crystals where the index of refraction depends on the polarization of the light on the material [3]. Light polarized parallel to the optical axis of the material experiences no birefringent effects. Light polarized at any other angle is split into two rays: the ordinary ray, which has a constant index of refraction, and the extraordinary ray, which has an index of refraction that depends on the propagation direction in the material [3]. The birefringence, Δn, of a material is defined as the difference between the indices of refraction experienced by these two rays,

$$\boldsymbol{\Delta n = n_e - n_o} \quad (1)$$

where n_e and n_o are the indices of refraction experienced by the extraordinary and ordinary rays, respectively [3]. When light is polarized perpendicular to the optical axis, the rays experience a difference in index of refraction but do not separate as they travel through the material. This means that birefringence can be measured by the phase difference between transmitted beams [2, 3].

Until 1979, attempts to measure VMB used variations on an interferometer to measure separately the indices of refraction parallel and perpendicular to the applied magnetic field to find the birefringence [2]. However, a more accurate measurement can be found using polarimetry to measure the phase difference between two components of the same light field rather than comparing separate beams [2]. The most advanced polarimetry experiment is the Polarizzazione del Vuoto con LASer (PVLAS) experiment, which uses a magnetic field of 2.3T

and a cavity length of 1.9m [1,2]. PVLAS has set an upper bound on VMB of $\Delta n_{PVLAS} = 4x10^{-23} /T^2$ [1]. This measurement level is within an order of magnitude of, but still above, the predicted VMB of $\Delta n_{QED} = 4x10^{-24} /T^2$ [1].

Another suggested experiment to measure VMB uses the proposed setup designed for the upcoming Any Light Particle Search II (ALPS-II) experiments [4]. Light particles beyond the Standard Model, such as axions, have been suggested as possible candidates for dark matter [4]. ALPS hopes to detect the presence of axions using a light shining through a wall experiment [5]. In this experiment, two optical cavities in vacuum tubes are separated by a solid wall in a magnetic field of 5T from a string of 12 HERA magnets on each side. When light resonates in the first cavity, the production cavity, a small fraction of photons interact with the high magnetic field, converting to axions. Because axions have very little interaction with matter, they can travel through the wall into a second cavity, the regeneration cavity, and magnetic field. Some small fraction of axions convert to identical photons of the same wavelength as in the production cavity. If the regeneration cavity is resonant to light of this wavelength, the probability of axion-to-photon conversion is greatly enhanced. Any light detected in the regeneration cavity must come from the conversion of axions [5]. The ALPS-I (2007-2010) experiment had the best detection limits of any previous experiment, but improvements in the optical resonator were identified that could improve the sensitivity [5]. To increase the sensitivity, the ALPS-II experiments place both cavities in the same vacuum tank, increases the magnetic length, and improves the detection system [5]. The length of the cavity, 100m, and high field, 5.3T, in the ALPS-IIc set-up make it a good candidate for measuring VMB [4]. Vacuum exhibits birefringence in a high magnetic field when photons in the incoming light field interact with virtual photons in the magnetic field [4]. The higher field in the ALPS-IIc setup increases the

birefringent effect of the vacuum [6]. The longer cavity length increases the magnitude of the phase difference in the resonant light and will hopefully increase the signal above the systematic errors in the system [3].

In any experiment to measure VMB, it is important to isolate the birefringence of the vacuum from the birefringence of the total optical system. Fluctuations in the mirror reflective coatings causes birefringence in the light beam, and systematic noise create signals that can obscure the signal from VMB. Therefore, in order to measure the small effect of VMB, the sources of noise in the proposed measurement technique must be identified and reduced. This paper outlines the set-up process and preliminary testing for measuring the birefringence of the optical cavity. I discuss the procedure to measure the beam for aligning light into an optical cavity, mode matching the cavity, creating controlled birefringence in the cavity, and measuring the phase differences in the light that interacts with the cavity.

Laser and Cavity Alignment

In this experiment, two lasers are incident on the cavity. Both lasers are 1064nm. The master laser frequency will be locked on resonance with the Fabry-Perot cavity, while the local oscillator (LO) Laser frequency will be locked to a frequency offset with the master laser using heterodyne locking. Each laser beam was passed through a Faraday isolator, a half-wave plate (HWP), and a polarizing beam splitter (Pol BS) to control the power transmitted from each laser and to prevent reflected light from re-entering the lasers. The beams were then combined on a power beam splitter (PBS) and one of the resultant beams was focused on a single mode optical fiber (Figure 1). The fiber matches the spatial modes of the two lasers, removes higher order modes, and produces a near-Gaussian beam at the other end [7].

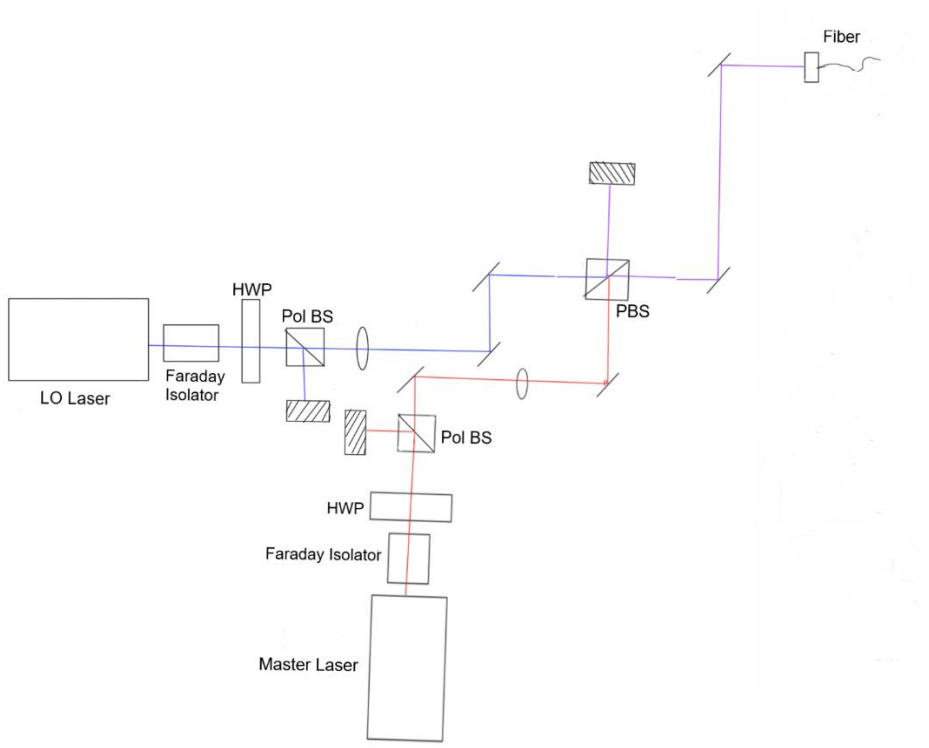

Figure 1: The diagram for the table-top setup for combining the laser beams into the fiber. The Faraday isolator in front of each laser prevents reflected from reentering the laser. The half-wave plate (HWP) and polarizing beam splitter (Pol BS) were used to control the power from each laser transmitted to the fiber. The beams were combined in a power beam splitter (PBS) before being steered into the single-mode fiber.

A Fabry-Perot cavity was built using two mirrors each with a radius of curvature (ROC) of 1m. The cavity was 0.66m long leading to a free spectral range of 227MHz. The finesse of the cavity was approximately 800. The output mirror was placed first, and a rough alignment was obtained by steering the retroreflection back along the initial path. Then, the input mirror was inserted. A PBS was placed before the input mirror and another after the output mirror, and the reflected beam was collected by a photodetector. The photodetector signal before the cavity (R

PD) is at a maximum when the laser is off resonance. When the laser is resonant, a majority of the light is transmitted through the cavity creating a maximum on the second photodetector (T PD). The second beam from the beam splitter was focused on a camera to observe the modes resonant in the cavity to assist with further cavity alignment and mode matching (Figure 2).

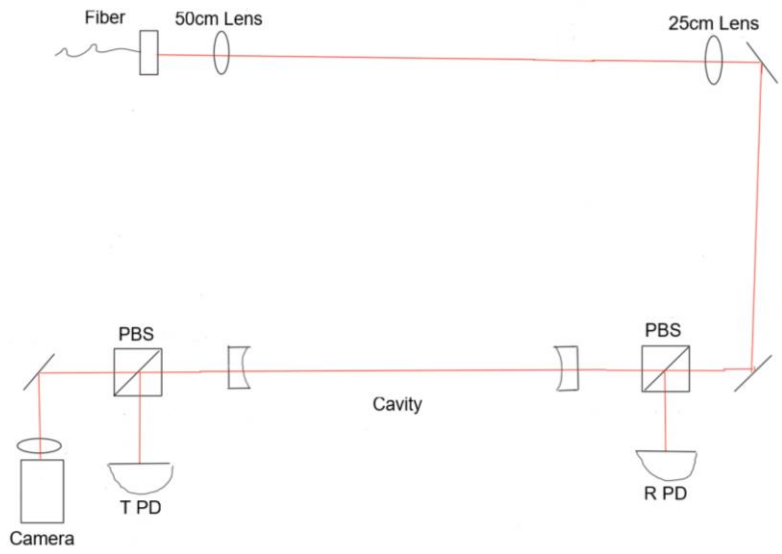

Figure 2: The cavity was built using two mirrors with a radius of curvature (ROC) of 1m. Light from the fiber was steered through a power beam splitter (PBS) and into the cavity. Light reflected from the cavity was measured with the reflected photodetector (R PD). The second beam from the PBS after the cavity is captured by a camera for mode matching. The lenses shown before the first steering mirror were used for mode matching and the process is explained in the next section.

Mode Matching

Gaussian modes are the simplest modes by which a laser beam can propagate through a medium [8]. As a Gaussian beam propagates it converges to minimum effective size at the waist and then diverges again. While the size of the beam changes during propagation, the shape remains consistent making the beam easier to analyze [8] (Figure 3a). The beam waist size is two times the waist radius and is defined as the width of the region where the intensity is at least 13.6% the maximum [9] (Figure 3b). The beam radius at any point along the propagation axis is

$$\boldsymbol{w(z) = w_0\sqrt{1 + \left(\frac{z - z_0}{z_R}\right)^2}} \tag{2}$$

and depends on the waist radius (w_0), distance from the waist location ($z - z_0$), and the Rayleigh range (z_R) [10]. The Rayleigh range is defined as the distance where the cross-sectional area of the beam has doubled or where the beam size has increased by $\sqrt{2}$ and can be calculated from the waist size and wavelength of light [9].

$$\boldsymbol{z_R = \frac{w_0^2 \pi}{\lambda}} \tag{3}$$

The wave front curvature of the beam is

$$\boldsymbol{R(z) = (z - z_0)\left[1 + \left(\frac{z_R}{z - z_0}\right)^2\right]} \tag{4}$$

The beam wavefront is in a plane at the waist location and picks up curvature as it propagates away from the waist [9,10].

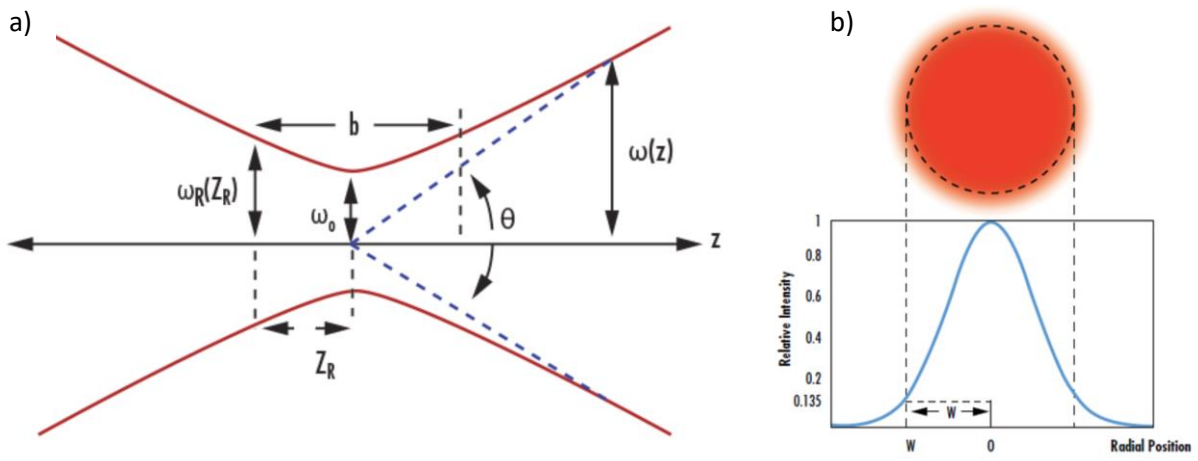

Figure 3: a) The red line shows a Gaussian beam profile. w(z) is the beam radius at any point along the propagation axis. The waist, w_0, is the narrowest point along the path. z_R is the Rayleigh range and is the distance from the waist location to where the beam cross-sectional area has doubled or w_0 has increased by $\sqrt{2}$ [10]. b) The Gaussian curve shows how intensity changes across the cross-section of the beam. The outer edge of the beam is defined as the point where the intensity is 13.6% of the maximum [9].

The modes present in the cavity can be seen using the dot patterns captured by the camera collecting the transmitted light. The patterns show which spatial modes are excited in the cavity. Ideally, the light will be concentrated in the lowest order mode, the 00 mode, and very little energy will be lost to higher-order modes. The patterns that have rectangular symmetry are Hermite-Gauss modes and are caused by beam or cavity alignment issues [11] (Figure 4a). These modes can be reduced by adjusting the steering mirrors to walk the beam across the input mirror. Other patterns form with radial symmetry, and these are Laguerre-Gauss modes [11] (Figure 4b). The order of these modes can be reduced by adjusting the shape of the input mirror with lenses to improve the mode matching of the beam with the cavity beam.

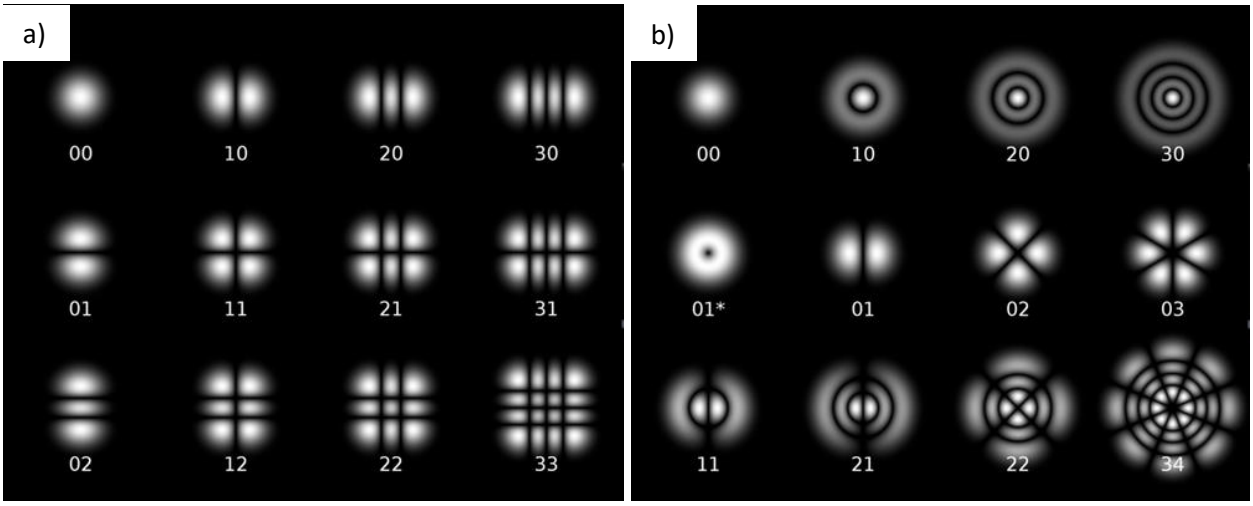

Figure 4: Two pattern types that show the resonant spatial modes in the cavity [11]. The purpose of alignment and mode matching is to reduce the power in higher-order modes excited in the cavity so that most of the light power incident on the cavity excites the lowest order 00 Gaussian mode. a) Strong, higher-order Hermite-Gauss modes indicate misalignment of the beam on the cavity mirrors. b) Strong, higher-order Laguerre-Gauss modes indicate mode mismatch between the laser beam and cavity beam.

In order to maximize the power in the 00 mode of the cavity, the propagation mode of the beam should match that supported by the cavity. Mode matching is the process of matching the beam modes through the addition of lenses or other optical elements. The complex beam parameter, or q-parameter, q, is used to compare the size and curvature of Gaussian beams [12]. If the q-parameters match, then both beams have the same mode. The q-parameter can be calculated as

$$\frac{\boldsymbol{1}}{\boldsymbol{q(z)}} = \frac{\boldsymbol{1}}{\boldsymbol{R(z)}} + \boldsymbol{i}\frac{\boldsymbol{\lambda}}{\boldsymbol{\pi w^2(z)}} \qquad (5)$$

The complex beam parameter can also be expressed using the Rayleigh range [12].

$$\boldsymbol{q(z) = z - iz_R} \quad (6)$$

Usually the incident laser beam must be adjusted through the addition of lenses to match the mode supported by the cavity. The effect of a medium or other optical element on the beam is calculated using ABCD matrices, with the generally form of $\begin{bmatrix} A & B \\ C & D \end{bmatrix}$ [12]. The matrix for the effect of a lens with focal length f is $\begin{bmatrix} 1 & 0 \\ \frac{-1}{f} & 1 \end{bmatrix}$. The change in the beam after propagating a distance d through a medium with an index of refraction n is calculated with the matrix $\begin{bmatrix} 1 & \frac{d}{n} \\ 0 & 1 \end{bmatrix}$, and the effect of a curved mirror with ROC R is $\begin{bmatrix} 1 & 0 \\ \frac{2}{R} & 1 \end{bmatrix}$ [12]. The matrices for each element the beam encounters as it propagates from the fiber to the cavity can be multiplied and used to find q', or the q-parameter of the beam after the effect of the element [12]

$$\boldsymbol{q'(z) = \frac{Aq(z) + B}{Cq(z) + D}} \quad (7)$$

The Rayleigh range for the cavity beam was calculated using Equation 4. The curvature of the beam must match the curvature of the cavity mirrors, meaning the beam had ROC of 1m at each mirror. The cavity was also symmetric, which placed the waist in the center of the cavity. Therefore, the distance between the waist and each mirror was half the cavity length, or 0.33m. With these values, the Rayleigh range of the cavity was calculated as 0.470m. The cavity waist was found to be $3.99x10^{-4}$m. This makes the q-parameter for the cavity at the waist location q(0) = 0.470i.

The next step was to characterize the beam transmitted from the fiber. The diameter of the beam from the fiber end coupler through the location of the waist was measured with a

WinCamD camera using DataRay software (Figure 5). The camera lens was placed in the beam path and the diameter was recorded every 3in. The waist diameter was found to be $8.5x10^{-4}$m at 1.5cm in front of the fiber.

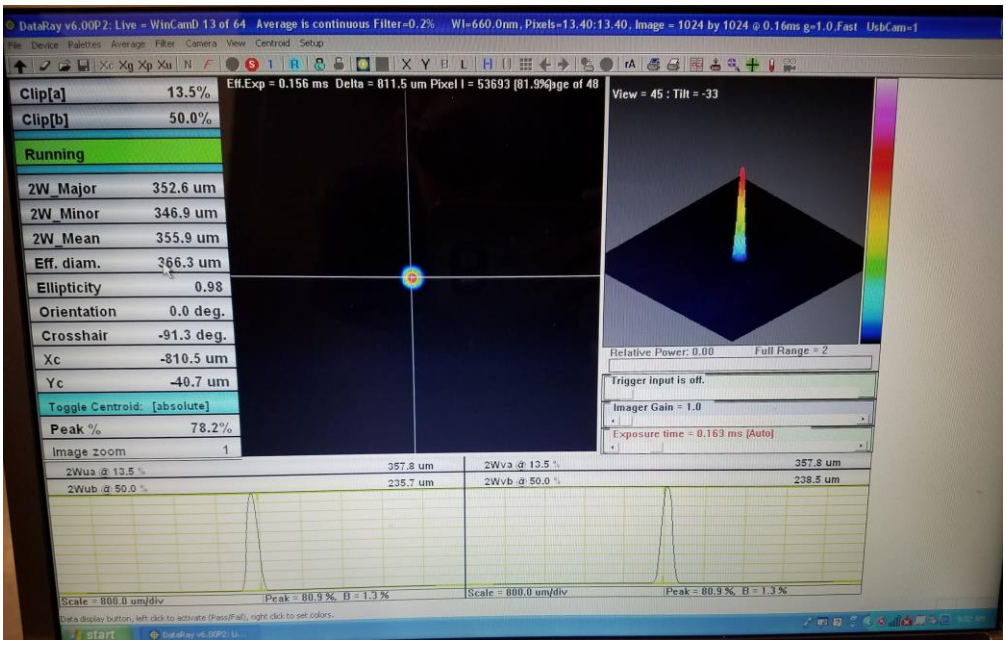

Figure 5: The beam size was measured using a WinCamD camera and DataRay software. The camera was placed into the beam and the effective diameter (Eff. diam.) was recorded. The beam size is the radius of the beam or half the diameter measured.

With the initial beam parameters, the beam could be modeled using JamMT, a java-based mode matching tool (Figure 6). The fiber end location was defined as z = 0. The waist size of $4.25x10^{-4}$m and a waist location of 1.5m were entered as the initial beam in the software. The input mirror of the cavity entered at its location of 1.3m from the fiber. Then, lenses were inserted in the beam path to observe the effect on beam shape. Inserting a 0.5m focal length lens 5mm from the fiber end and a 0.25m lens 70mm from the fiber created a final beam that most

closely matched the cavity beam. The lenses were placed in the actual beam path and the lens location was fine-tuned to reduce the number of higher order modes visible on the camera.

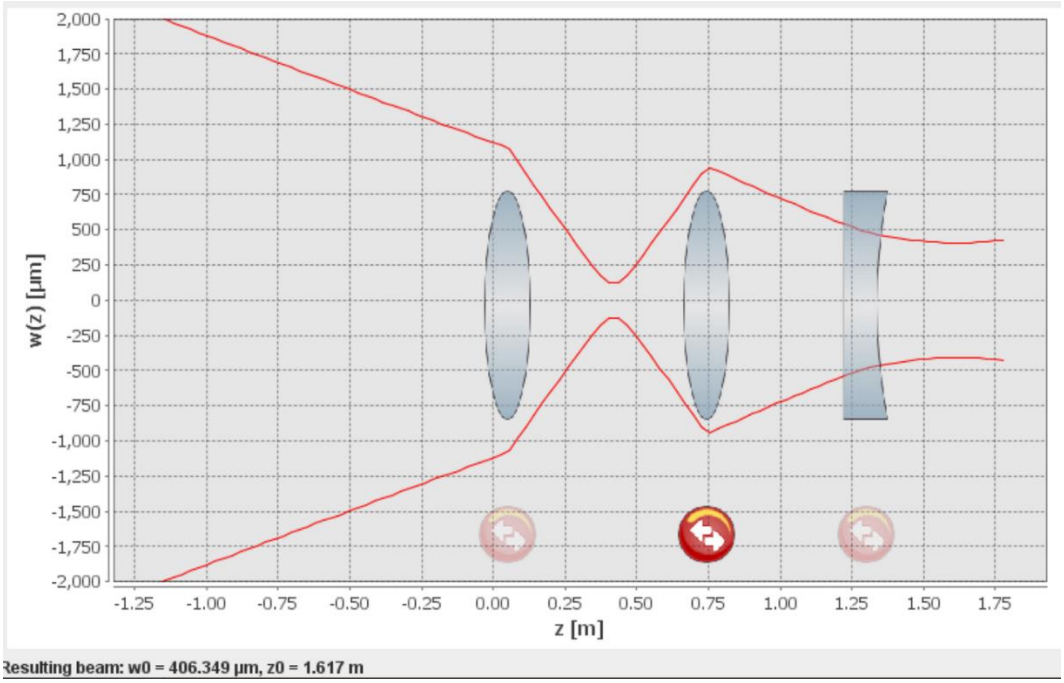

Figure 6: The beam waist and location from the fiber end were entered in the Java-based mode matching tool JamMT. The cavity input mirror was also placed at its distance from the fiber. Then, lenses were added to change the input beam parameters to match the calculated cavity parameters.

The size of the beam with the effect of the lenses was measured using a beam chopper. The chopper wheel is placed so that the blades cut through the laser beam, and the transmitted beam is collected with a photodetector. The photodetector signal displayed on an oscilloscope is the integral of the Gaussian beam profile (Figure 7). The beam size is proportional to the rise time between the 13.6% and 86.4% voltage points [13]. The 10-90 rise time measurement from the oscilloscope can be used with a correction factor. The beam size is

$$w = 0.7803 * 2\pi Rf\tau \quad (8)$$

where R is the distance between the center of the chopper wheel and where the beam intersects the blades, f is the frequency from the chopper controller, and τ is the 10-90 rise time [13].

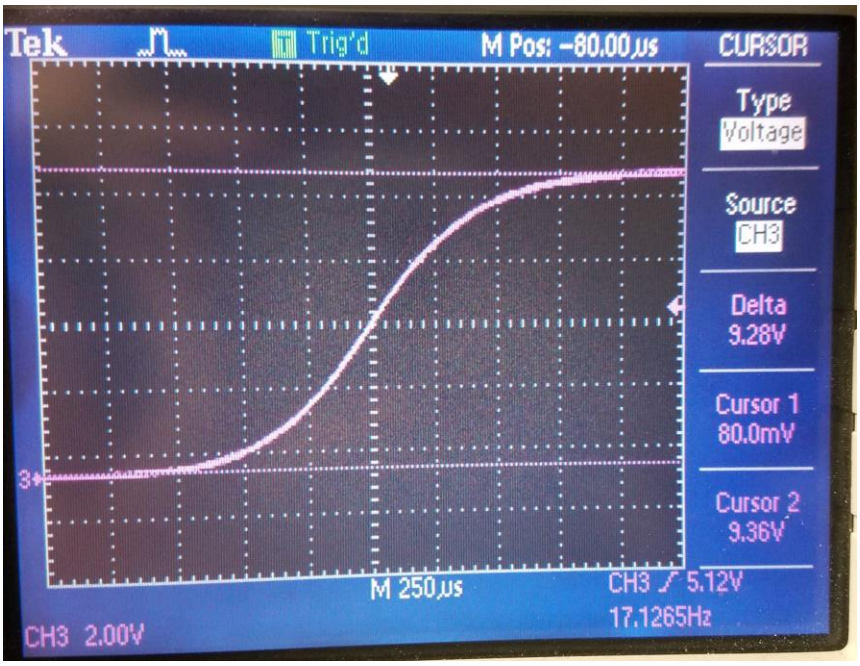

Figure 7: The integrated beam profile from the beam chopper measurements displayed on the oscilloscope. The signal is at zero when the beam is blocked by the chopper blade and increases as the blade spins through the beam until all of the beam is able to pass to the photodetector. The beam size is proportional to the time for the signal to rise from 13.6% to 86.4% of the maximum voltage. The 10-90 rise time value from the oscilloscope can also be used with a correction factor.

The beam radius was graphed against distance from the fiber coupler, and Equation 2 was fitted to the data using least-square regression in Excel (Figure 8). The waist size of the fitted curve was 4.12×10^{-4}m at 167cm from the fiber. The effect of the input mirror was then

calculated using the q-parameter using the definition if Equation 6. The q-parameter of the fiber beam at its waist location is q(0) = 0.501i. The beam is then propagated 0.37m back through air to in front of the input mirror location. The beam was propagated through the mirror and 0.33m forward to the location of the cavity waist. The q-parameter of the fiber was q(0.33) = 0.672i + 0.068, which translates to beam parameters after the mirror of a waist of $4.77\text{x}10^{-4}$m at 157cm from the fiber. The fiber beam matches closely to the cavity beam with a waist of $3.99\text{x}10^{-4}$m at 163cm from the fiber. The fiber beam size with the effect of the mirror was calculated and graphed in Excel (Figure 9). The mismatch between the corrected fiber beam and the cavity was calculated using

$$\left(\frac{\Delta w}{w}\right)^2 + \left(\frac{\Delta z}{2z_R}\right)^2 \tag{8}$$

where Δw is the difference in waist size between the beams, and Δz is the difference between waist location. The mismatch was found to be under 1%.

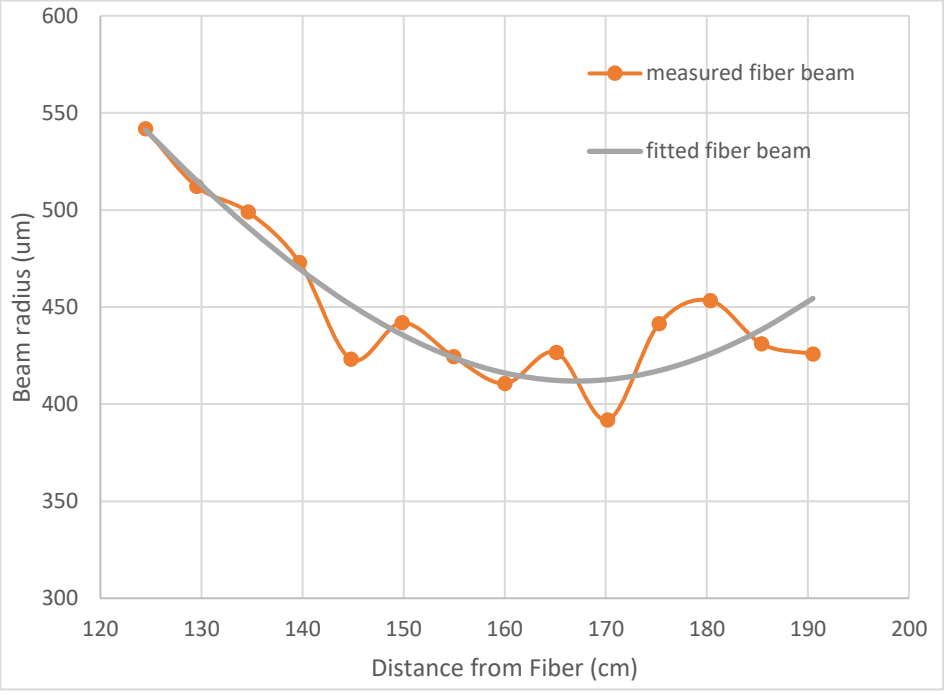

Figure 8: The orange line is the radius of the beam measure using a beam chopper graphed along distance from the fiber. The grey line is the least squares fit of the data to Equation 2. From the fit line, the beam waist was $4.12x10^{-4}$m at 167cm from the fiber.

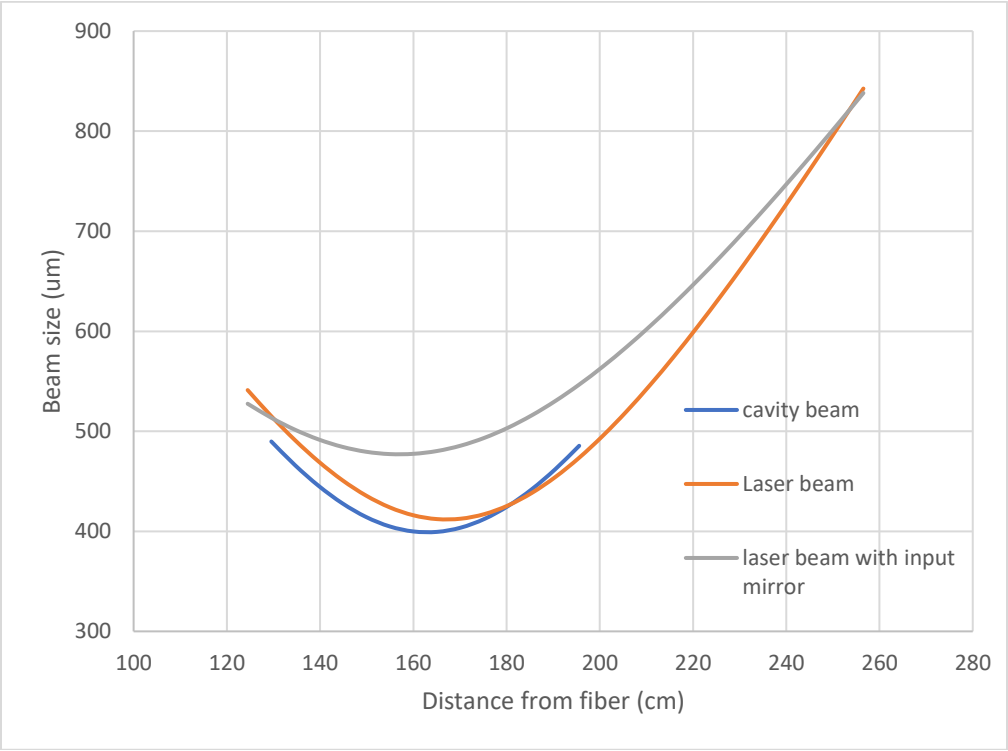

Figure 9: The beam size is graphed against the distance of the beam from the fiber end. The blue line is calculated cavity beam using Equation 2. The grey line shows the fitted curve from chopper data measured without the cavity input mirror in the beam path. The effect of the input mirror was determined using complex beam parameters, q, describe the beam shape and ABCD matrices to calculate the effect of the mirror and beam propagation on beam parameters. The orange line was calculated from the beam parameters, taking into account the first cavity mirror.

The mode matching was confirmed using the modes visible on the camera. The 00 mode was by far the brightest mode observed, and the other visible modes were all lower order Laguerre-Gaussian modes (Figure 10a-d). The power in each mode was quantified by measuring

transmitted power from the cavity as the slow controller of the laser is swept over at least one free spectral range (FSR) of the cavity (Figure 11a-b). Since the voltage from a photodetector is proportional to the power incident on it, the voltage peaks on an oscilloscope describe the relative power in each mode. The 00 mode peaks are 5.2V while the peaks from the other modes total 50mV. This shows that 99% of the power is in the 00 mode.

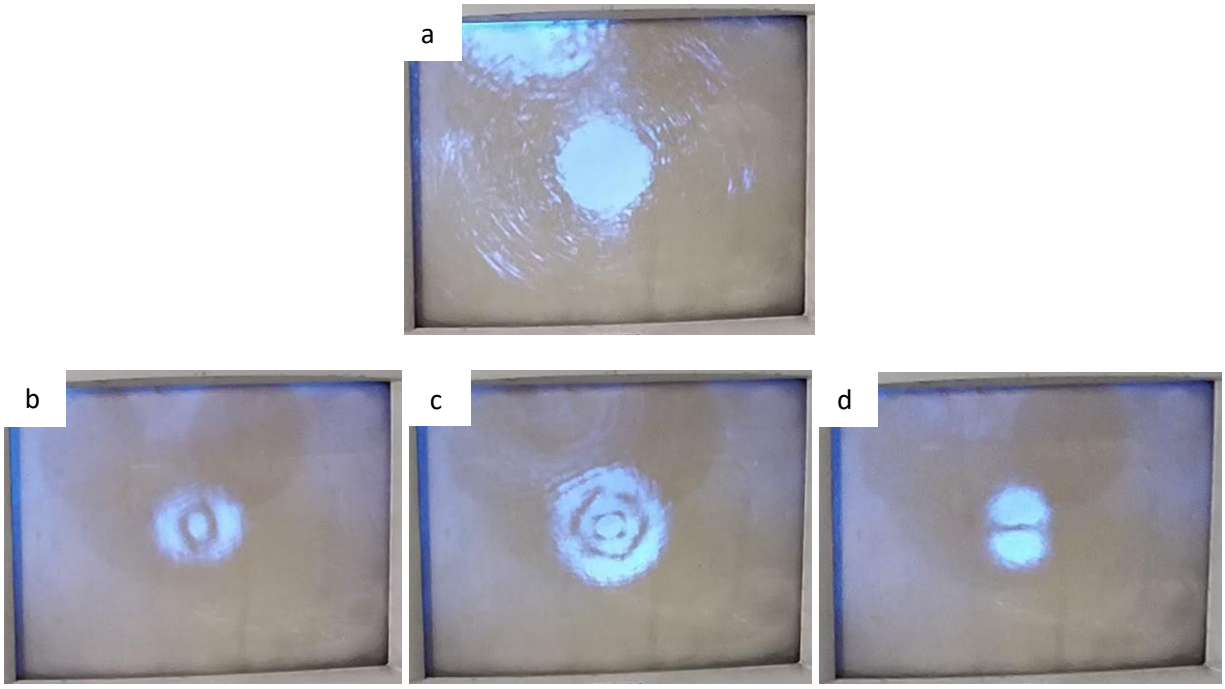

Figure 10: The image from the camera was displayed on a TV to see the patterns formed by the resonant modes in the cavity. a) The 00 mode was the brightest mode in the cavity. b) 10 mode. c) 20 mode. d) 01 mode. The higher order modes were all Laguerre-Gauss mode matching modes. However, since all these modes were dimmer than the 00 mode and none of them were higher than second order, the cavity is very well mode matched.

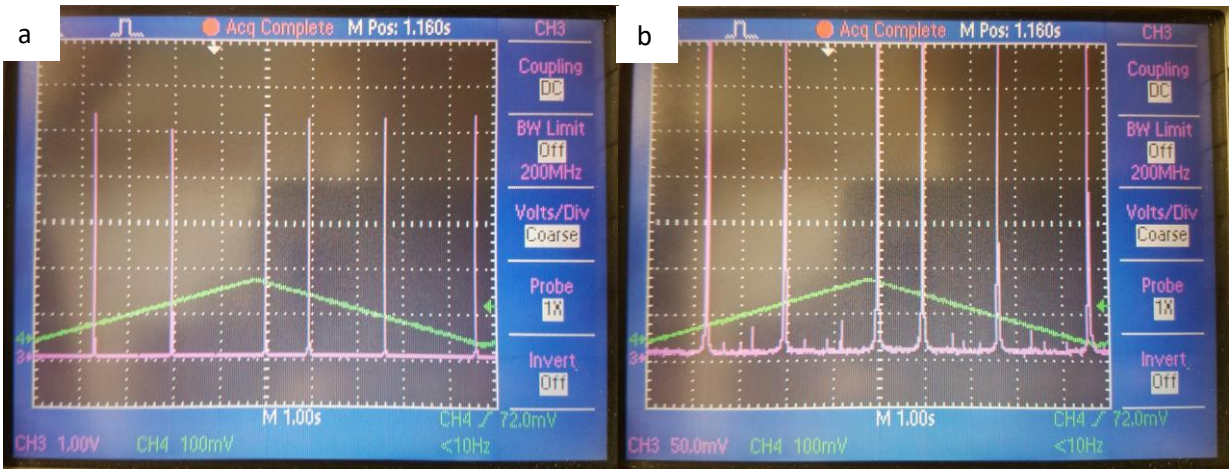

Figure 11: The transmitted photodetector signal is displayed on an oscilloscope along with the voltage that was applied to the slow control of the laser to sweep across two FSRs of the cavity. The peaks show the places where the light was on resonance with the cavity. a) The peaks from the 00 mode were 5.2V high. b) The higher order mode peaks total 50mV. Since the voltage is proportional to the power in the modes, 99% of the power is resonant in the 00 mode.

Measuring Cavity Birefringence

The end mirror of the cavity on the table was replaced with a short Fabry-Perot cavity built on an ultra-low expansion (ULE) glass substrate to reduce thermal length fluctuations (Figure 11). A PBS before the input mirror separates a beam that does not interact with the cavity, and this reference beat note is collected by the Ref PD. The other beam passes through a rotating HWP at frequency, f, of 5Hz which rotates the polarization of light incident on the cavity at a frequency of 4f or 20Hz. Light reflected from the cavity is split by a Pol BS. The p-polarization light (P PD) is used to lock the master laser to the cavity. The s-polarized light (S PD) is used to measure the birefringence of the cavity. Since the p-component of the light is held on resonance with the cavity, the s-polarization alternates to either side of resonance. The phase of the light oscillates with a frequency of 4f and the amplitude is proportional to birefringence of

the cavity. Phase data was collected with the Moku:Lab phasemeter. The phase difference between the Ref PD and S PD was analyzed. Any change in phase in both signals is from noise in the system and is cancelled out. Phase changes in just the S PD signal is the result of birefringence.

The master laser was locked to the main cavity using a variation of the Pound-Drever-Hall (PDH) technique [14] where the sidebands on the carrier frequency were generated by modulating the fast control on the laser with a 1MHz signal and 10mVpp. The error signal was created by mixing the Ref PD and P PD and passing the signal through a low-pass filter. The LO laser was locked to the master laser to a beat note frequency of 25MHz using heterodyne polarimetry [15]. The error signal was generated using a function generator set to 25MHz.

Controlled birefringence was added to the cavity by actuating the end mirror of the short end cavity with a piezo element. The mirror was modulated using a function generator applying a sinusoidal voltage on the piezo actuator at 2Hz and 2.5Vpp with a 2.5V offset. Small fluctuations in the cavity length bring the light into and out of resonance, creating small changes in phase as the light travels different distances in the cavity. To create birefringence, only one polarization should experience this change in phase. By inserting a polarizer in between the end mirrors, only one polarization can interact with the cavity.

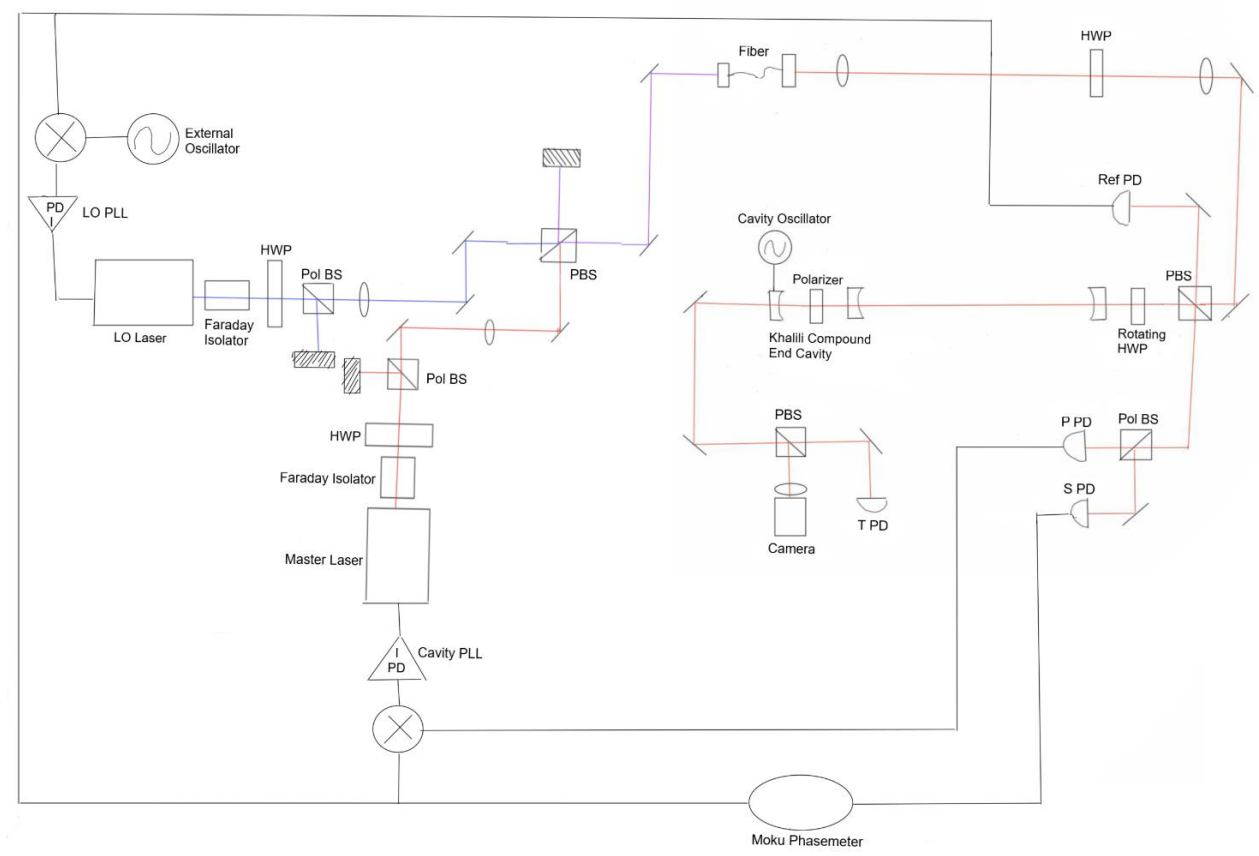

Figure 11: Two lasers, the master laser and the local oscillator (LO) laser were combined into an optical fiber. The beam from the fiber was steered into an optical cavity. The input mirror was a mirror with a radius of curvature (ROC) of 1m. The end mirror of the cavity was replaced with a short Fabry-Perot cavity with a piezo actuated end mirror, and this was used to add time dependent birefringence to the cavity. The master laser was locked with Pound-Drever-Hall (PHD) locking, and the LO laser was locked to a 25MHz beat note with the master laser using laser heterodyne locking. A power beam splitter (PBS) before the cavity input mirror separated a reference beam that did not interact with the cavity and the signal was collected by a photodetector (Ref PD). Light reflected from the cavity was separated based on polarization using a polarizing beam splitter (Pol BS). The p-polarization was used to lock the master laser to the cavity (P PD). The s-polarization (S PD) was combined with the Ref PD in the Moku:Lab

phasemeter. The phase difference between the two signals was used to determine the birefringence of the cavity. The rotating half wave plate (HWP) before the cavity rotated the polarization of the light on the cavity. Because the p-polarization was locked on resonance, the s-polarization was oscillated across resonance at a rate of 20Hz or four times the rotation speed of the HWP.

Results

The initial testing show the expected phase behavior. The phase difference was graphed against frequency (Figure 12). There was a peak at 20Hz, which is the rotation frequency of the s-polarized light around resonance. There are also peaks at 18 and 22Hz which shows the birefringent effect caused by the 2Hz modulation of the end Khalili mirror. The peaks at other frequencies are at other frequencies are systematic noise.

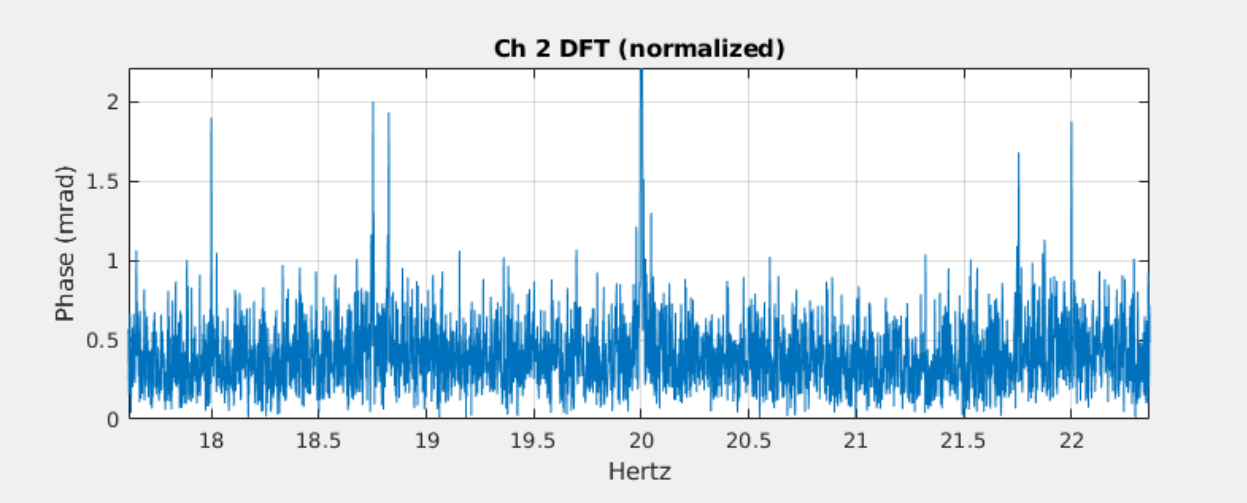

Figure 12: The phase difference between the Ref PD and the S PD beat notes was graphed in the frequency domain. The phase shows a large 60mrad peak at the expected 20Hz or four times the rotation speed of the HWP before the cavity. Side band peaks are visible at 18Hz and 22Hz and show the change in cavity birefringence due to the modulation of the piezo element at 2Hz.

Future Testing

The setup for a measuring vacuum magnetic birefringence using heterodyne polarimetry and ALPS hardware was tested. A cavity was built and mode matched. The end mirror of the cavity was replaced by a short cavity with a piezo actuated end mirror. The proposed method to simulate birefringence without a magnetic field with this end cavity was confirmed in initial testing.

In future testing, systematic noise will be identified and reduced so that the birefringence signal is not obscured. Both lasers could be locked at the same time, but not with very stable locks. Increasing the time the lasers are locked by adjusting control loop parameters will allow data to be collected for longer periods of time and so reduce the magnitude of constant, systematic noise. The short end cavity is likely not on anti-resonance. To find this point, the piezo will be connected to a voltage generator, and a constant voltage will be applied while phase data is collected. Anti-resonance is where the greatest change in birefringence with applied voltage is found. Then, a modulated sinusoidal signal to the piezo actuator centered around anti-resonance to find the relationship between magnitude of modulated birefringence and the magnitude of the measured signal.

Acknowledgements

I would like to extend a huge thank you to my mentor Hal Hollis for teaching me so much this summer. Thank you to my advisors Professor Guido Mueller and Professor David Tanner for all your advice. And thank you to the members of the ALPS, LIGO, and LISA groups for always being willing to lend a hand.

I would also like to thank Professor Selman Hershfield and the Department of Physics at the University of Florida for making this amazing experience possible. This work was funded by NSF grant DMR-1852138.

References

1. F. Della Valle, et al, First results from the new PVLAS apparatus: a new limit on vacuum magnetic birefringence, arXiv:1406.6518, (2014).
2. M. T. Hartman, A. Rivèrea, R. Battesti, and C. Rizzo, Noise characterization for resonantly enhanced polarimetric vacuum magnetic-birefringence experiments, Review of Scientific Instruments **88**, 123114 (2017).
3. D. B. Murphy, K. R. Spring, T. J. Fellers, and M. W. Davidson, Principles of Birefringence, MicroscopyU, Nikon Instruments, Inc, (2019).
4. K. Ehert, The ALPS Light Shining Through a Wall Experiment - WISP Search in the Laboratory, ALPS Collaboration, Deutsches Elektronen-Synchrotron DESY, arXiv:1006.5741, (2010).
5. https://alps.desy.de/
6. A, Ejlli, F. Della Valle, G. Zavattini, Polarisation dynamics of a birefringent Fabry-Perot cavity, arXiv:1707.02967v1, (2017).
7. https://www.rp-photonics.com/mode_cleaners.html

8. https://www.rp-photonics.com/modes.html
9. https://www.edmundoptics.com/resources/application-notes/lasers/gaussian-beam-propagation/
10. https://www.edmundoptics.com/resources/tech-tools/gaussian-beams/
11. http://www.optique-ingenieur.org/en/courses/OPI_ang_M01_C03/co/Contenu_14.html
12. Anthony E Siegman, Lasers, University Science Books, pp. 639-640, 785-791, (1986).
13. http://citeseerx.ist.psu.edu/viewdoc/download?doi=10.1.1.215.6234&rep=rep1&type=pdf
14. D Black, An introduction to Pound-Drever-Hall laser frequency stabilization, American Journal of Physics **69**, 79 (2001).
15. H. Hollis, G. Alberts, D. B. Tanner, G. Mueller, A laser heterodyne polarimeter for birefringence measurement, arXiv:1710.03801, (2019).